The exterior gravitational potential of toroids

J.-M. Huré, B. Basillais, V. Karas, A. Trova, O. Semerák

Monthly Notices
of the
ROYAL ASTRONOMICAL SOCIETY

MNRAS **494,** 5825–5838 (2020)
Advance Access publication 2020 April 24

doi:10.1093/mnras/staa980

The exterior gravitational potential of toroids

J.-M. Huré,[1]★ B. Basillais,[1] V. Karas,[2] A. Trova[3] and O. Semerák[4]

[1]*Laboratoire d'Astrophysique de Bordeaux, Université de Bordeaux, CNRS, B18N, Allée Geoffroy Saint-Hilaire, F-33615 Pessac, France*
[2]*Astronomical Institute, Academy of Sciences, Boční II 1401, CZ-14100 Prague, Czech Republic*
[3]*Center of Applied Space Technology and Microgravity (ZARM), University of Bremen, D-28359 Bremen, Germany*
[4]*Institute of Theoretical Physics, Faculty of Mathematics and Physics, Charles University, CZ-180 00 Prague, Czech Republic*

Accepted 2020 March 23. Received 2020 March 23; in original form 2019 November 8

ABSTRACT

We perform a bivariate Taylor expansion of the axisymmetric Green function in order to determine the exterior potential of a static thin toroidal shell having a circular section, as given by the Laplace equation. This expansion, performed at the centre of the section, consists in an infinite series in the powers of the minor-to-major radius ratio e of the shell. It is appropriate for a solid, homogeneous torus, as well as for inhomogeneous bodies (the case of a core stratification is considered). We show that the leading term is identical to the potential of a loop having the same main radius and the same mass – this 'similarity' is shown to hold in the $\mathcal{O}(e^2)$ order. The series converges very well, especially close to the surface of the toroid where the average relative precision is $\sim 10^{-3}$ for $e = 0.1$ at order zero, and as low as a few 10^{-6} at second order. The Laplace equation is satisfied *exactly* in every order, so no extra density is induced by truncation. The gravitational acceleration, important in dynamical studies, is reproduced with the same accuracy. The technique also applies to the magnetic potential and field generated by azimuthal currents as met in terrestrial and astrophysical plasmas.

Key words: gravitation – methods: analytical – methods: numerical.

1 INTRODUCTION

The derivation of reliable and compact expressions for the gravitational potential of massive toroids is a longstanding problem of dynamical astronomy, from planetary to galactic scales. This is essential to not only examine the motion of test particles and fluids orbiting around, in the classical framework as well as in general relativity (Nieto 2005; Šubr & Karas 2005; Semerák & Suková 2010; Tresaco, Elipe & Riaguas 2011; Iorio 2012), but also understand the conditions for the formation, evolution, and stability of toroids themselves (Dyson 1893; Hachisu 1986; Chandrasekhar 1987; Tohline & Hachisu 1990; Woodward, Sankaran & Tohline 1992; Christodoulou 1993; Eriguchi & Mueller 1993; Hashimoto et al. 1993; Storzer 1993; Nishida & Eriguchi 1994; Pickett, Durisen & Link 1997; Horedt 2004; Lehmann, Schmidt & Salo 2019). While it is relatively easy to deduce the mass density corresponding to a given potential (e.g. Binney & Tremaine 1987), the inverse procedure is very complicated by analytical means, and it is almost impossible to go beyond the classical series representations and to get closed forms (Clement 1974; Cohl et al. 2001; Petroff & Horatschek 2008). Fully numerical approaches may be preferred for their apparent simplicity, but the computing times are generally large, often prohibitive at high spatial resolution, especially for very inhomogeneous configurations and/or very extended systems like discs. The numerical accuracy of discretization schemes is mainly limited when treating thin sources (having less than three spatial dimensions) whose field typically suffers a certain irregularity at their position.

In axial symmetry, the Green function $\mathcal{G}(\vec{r}|\vec{r}')$ of the Poisson equation involves the complete elliptic integral of the first kind **K** whose argument (or modulus) gathers all the pertinent variables (Kellogg 1929; Durand 1953; Fukushima 2016). The presence of a special function is a real obstacle when it is to be convolved with any non-trivial mass density $\rho(\vec{r}')$. One can overcome this difficulty by expanding **K** over the modulus, but the 'dual' nature of the series – different for large and for short separations – means piece-wise approximations whose connection requires technical efforts. This is done for instance in Bannikova, Vakulik & Shulga (2011), who match together the internal and the external potentials of the solid (i.e. homogeneous) torus from a minimization procedure.

This article brings a new contribution to this general and challenging problem. It is inspired by Huré et al. (2019), who derived a reliable approximation for the *interior* potential of a toroidal shell of circular cross-section, based on a bivariate expansion performed at the pole (or focal ring) of the toroidal coordinates. At this singular point, all the partial derivatives of the Green function are exceptionally analytical. Unfortunately, the 'pole' method does not apply outside the shell cavity because the line segment linking the focal ring to any exterior point crosses the shell where the Green function is basically singular. We generate accurate approximations for the *exterior* solution of the toroidal shell by expanding the

★ E-mail: jean-marc.hure@u-bordeaux.fr

axisymmetric Green function as a Taylor series *before integrating over the source*. As for the classical multipole expansion, the shell potential writes as an infinite series (e.g. Majic 2020), but our approach differs in that the origin of coordinates does not play a special role: the expansion is performed at the centre of the toroid section. Such an approach has been reported very recently by Kondratyev (2018) in the case of the solid torus. The author writes the external potential in the form $\sum_n \phi_n e^{2n}$ (e is the minor-to-major radius ratio, i.e. the torus parameter). He then uses the second-order expression to set constraints on the masses of thin, virialized rings orbiting an asteroid.

In this article, we go beyond the hypothesis made in Bannikova et al. (2011) and in Kondratyev (2018) by considering inhomogeneous systems too. In particular, we show that, when the toroid is radially stratified from the centre to the surface, only moments of the density need to be calculated. The method has an unexpected efficiency, not only at large distances but also quite close to the surface of the toroid. The leading term has a correct behaviour at infinity as well as on the Z-axis, and it obeys the Laplace equation. As a matter of fact, these desirable properties are shared by *all* terms of the expansion. There is thus no spurious noise or extra density induced in space, whatever the truncation order. We treat orders 0 to 2 explicitly (a driver F90 program is appended). The resulting shell potential can be recast in the form of a 'modified monopole' or in the form of an 'equivalent loop', which concept has been discussed in Stahler (1983), while proofs are found in Bannikova et al. (2011) and Kondratyev (2018). We show that the exterior potential of the solid torus, which is of more astrophysical relevance than the shell, is easily deduced, with all the properties observed for the shell maintained. The method also applies to the determination of the vector potential and magnetic field of electromagnetism for toroids carrying a purely azimuthal current (Trova et al. 2018).

The paper is organized as follows. In Section 2, the expression for the potential of a toroidal shell is given in its integral form. The axisymmetric Green function is expanded, in a bivariate manner, in Section 3. The leading term is calculated and compared with the potential of a monopole (i.e. a point mass) and of a circular loop. Its precision is checked against an 'exact' numerical reference in Section 4. The first-order and second-order approximations are then treated similarly in Section 5. In Section 6, we show how the exterior and interior solutions match together at the shell surface. The procedure leading to the nth-order term is detailed in Section 7. The case of a solid torus is treated in Section 8, while the case of core-stratified toroids is the aim of Section 9. The formula for the gravitational acceleration is derived in Section 10. In particular, we show that the vertical component that rules hydrostatic equilibrium differs by a factor of about 2 from Paczynski's estimate valid for thin discs (Paczynski 1978). This result is suited to examining the stability of rings (e.g. Wisdom & Tremaine 1988). From the radial component, we deduce the circular velocity of test particles orbiting in the equatorial plane. This formula can be helpful in explaining the deviations to the Kepler's law in massive systems (e.g. Guilloteau, Dutrey & Simon 1999). Section 11 is devoted to the magnetic potential due to toroidal currents (the leading term is derived). Two general comments are found in Section 12. Conclusions and perspectives are found in the last section.

2 POTENTIAL OF THE TOROIDAL SHELL

We consider the simplest possible toroidal shell, as depicted in Fig. 1. The major radius is R_c and the meridional section is circular,

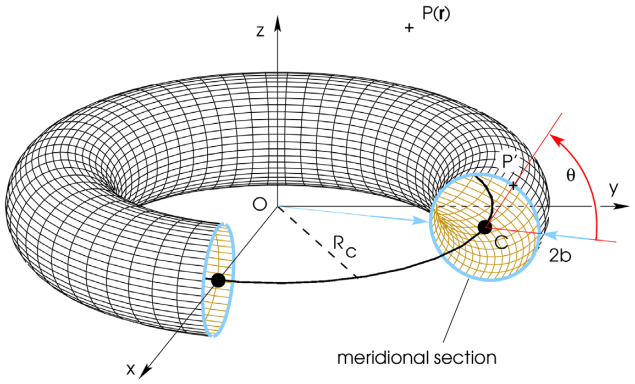

Figure 1. The infinitely thin, toroidal shell (main centre O and main radius R_c) with a circular meridional section (centre C and core radius b).

with centre C and minor radius

$$b \equiv eR_c \leq R_c, \tag{1}$$

where $e \in [0, 1]$ denotes the shell parameter. We work in cylindrical coordinates (R, Z), using the symmetry axis of the shell as the Z-axis, and xOy as the plane of symmetry. For this specific problem, the Green function of the Poisson equation (e.g. Kellogg 1929; Durand 1953) is

$$\mathcal{G}(R, Z; a, z) = -2\sqrt{\frac{a}{R}}k\mathbf{K}(k), \tag{2}$$

where

$$\mathbf{K}(k) = \int_0^{\frac{\pi}{2}} \frac{d\vartheta}{\sqrt{1 - k^2 \sin^2 \vartheta}} \tag{3}$$

is the complete elliptic integral of the first kind,

$$k = \frac{2\sqrt{aR}}{\Delta} \in [0, 1] \tag{4}$$

is its modulus, and

$$\Delta^2 = (R + a)^2 + \zeta^2, \tag{5}$$

where $\zeta = Z - z$, and (a, z) are the cylindrical coordinates of any point P′ belonging to the shell. Basically, equation (2) corresponds to the potential created by an infinitesimally thin circular ring with unit mass per unit length, radius a, and altitude z. This function is known to be logarithmically singular at the location of the ring (where $k \to 1$). The gravitational potential generated, at any point P$(\vec{r})$ of space, by such axisymmetric shell is then given by the integral

$$\Psi(\vec{r}) = -2G \int_0^{2\pi} \Sigma(\ell)\sqrt{\frac{a}{R}}k\mathbf{K}(k)d\ell, \tag{6}$$

where Σ is the local surface density, and $d\ell$ is the infinitesimal length along the shell section. In the case of a shell with a circular section of radius R_c, a and z are simply given by

$$a = R_c + b\cos\theta, \qquad z = b\sin\theta, \tag{7}$$

where $\theta \in [0, 2\pi]$ is the angular position of any point P′ on the shell with respect to the equatorial plane (see Fig. 1). The infinitesimal length then takes its simplest form, namely $d\ell = bd\theta$. Other options are possible, but the subsequent calculations are much more complicated (see Section 12).

The surface density Σ may be variable in local latitude θ. However, even if it is independent of θ, equation (6) cannot in

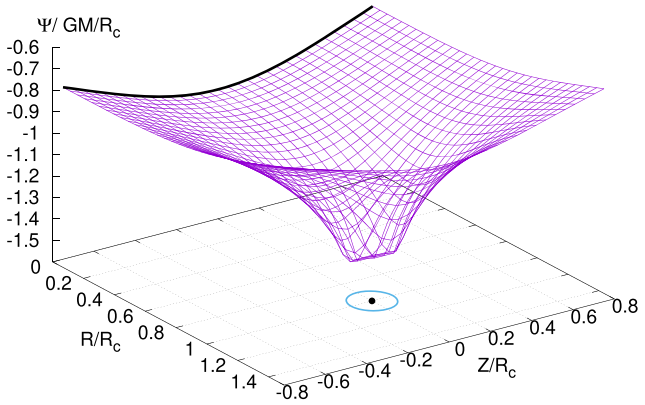

Figure 2. The gravitational potential of the toroidal shell in units of GM/R_c (homogeneous case) obtained by direct numerical computation of the integral in equation (6). The axis is in units of the main radius R_c. The normalized core radius (or shell parameter) is $e \equiv b/R_c = 0.1$. Also shown are the values on the Z-axis from the formula by Šácha & Semerák (2005) (*thick black line*), the projected shell section (*blue line*), and its centre C (*black dot*); see also Fig. 1.

general be integrated into a compact form, except on the Z-axis (Šácha & Semerák 2005). An example of a direct numerical estimate of Ψ is given in Fig. 2 for $e = 0.1$. We use the trapezoidal rule as the quadrature scheme. We will use such a numerical potential, denoted $\Psi_{\rm ref}$ in the following, as a 'reference' against which we will compare our approximations. As shown in Huré et al. (2019), the potential inside the shell cavity is a quasi-linear function of the cylindrical radius R, and it is weakly sensitive to the Z-coordinate, especially when $e \ll 1$. We see that the potential outside the cavity has a more complex structure. It resembles the potential of a loop, as already pointed out (e.g. Wong 1973; Bannikova et al. 2011; Kondratyev 2018).

3 EXPANSION OF THE GREEN FUNCTION. ZERO-ORDER FORMULA

As quoted in the introduction, the elliptic integral $\mathbf{K}$ may be expanded over k at $k \to 0$, which means far away from the source or close to the Z-axis, and over $k' = \sqrt{1-k^2}$ at $k \to 1$, e.g. close to or even inside the source (see e.g. Abramowitz & Stegun 1964; Gradshteyn & Ryzhik 2007). However, such two series have to be matched somewhere (Bannikova et al. 2011). In the present paper, we propose a more synthetic approach that consists in expanding the axisymmetric Green function over a and z, before integration over θ in equation (6). We expect to preserve the asymptotic behaviour of the potential at large distances. Let us remind that, for any 'regular enough' function f of two independent variables x and y, the bivariate Taylor expansion at (x_0, y_0) writes

$$f(x,y) = f(x_0,y_0) + \sum_{n=1}^{\infty} \frac{1}{n!} \left\{ \left[(x-x_0)\frac{\partial}{\partial x'} + (y-y_0)\frac{\partial}{\partial y'} \right]^n f(x',y') \right\}_{\substack{x'=x_0 \\ y'=y_0}}. \quad (8)$$

The expansion is performed in $x \equiv a$ and $y \equiv z$, at the centre C of the shell, i.e. at $x_0 \equiv R_c$ and $y_0 \equiv 0$ (see Section 12 for the expansion at the focal ring). We see from equation (7) that this is valid for $e < 1$, which in astrophysical toroids (typically orbiting a massive central body) is safely satisfied.

In fact, it is not necessary to expand the whole Green function. In particular, the term $\sqrt{a}$ is not problematic and it can be left aside. There are several options. For instance, if we expand $k\mathbf{K}(k)$ or $\mathbf{K}(k)$, the subsequent integration over θ will generate a new series of elliptic integrals (again, see Section 12). That is not a problem per se, but it complicates the calculations when the solid torus is considered. Seeing that the complication can be avoided when extracting the other factor $\sqrt{a}$ contained in the modulus equation (4), we finally choose to expand

$$\frac{\mathbf{K}(k)}{\Delta} \equiv \kappa \quad (9)$$

as

$$\kappa = \kappa|_{\substack{a=R_c \\ z=0}} + (a-R_c)\left.\frac{\partial\kappa}{\partial a}\right|_{\substack{a=R_c \\ z=0}} + z\left.\frac{\partial\kappa}{\partial z}\right|_{\substack{a=R_c \\ z=0}} + \frac{1}{2}(a-R_c)^2\left.\frac{\partial^2\kappa}{\partial a^2}\right|_{\substack{a=R_c \\ z=0}} + (a-R_c)z\left.\frac{\partial^2\kappa}{\partial a\partial z}\right|_{\substack{a=R_c \\ z=0}} + \frac{1}{2}z^2\left.\frac{\partial^2\kappa}{\partial a\partial z}\right|_{\substack{a=R_c \\ z=0}} + \dots. \quad (10)$$

Note that κ is nothing but the axisymmetric Green function, i.e. $\oint |\vec{r}-\vec{r}'|^{-1} d\phi$. Since it is a function of a, z, R, and Z, the infinite series is a polynomial (of 'infinite' degree) in a and z, whose coefficients are functions of R and Z. This series naturally exhibits powers of the shell parameter e, which come from the partial derivatives and from the terms $a - R_c$ and z as well; see equation (7). With equation (10), equation (6) becomes, at the lowest (zeroth) order

$$\Psi(\vec{r}) \approx -4G\Sigma_0\kappa_0 b \times 2\pi R_c S_{0,0} \equiv \Psi_0(\vec{r}), \quad (11)$$

where

$${k_0}^2 = \frac{4R_cR}{\Delta_0^2}, \quad (12)$$

$$\Delta_0^2 = (R+R_c)^2 + Z^2, \quad (13)$$

$$\kappa_0 = \frac{\mathbf{K}(k_0)}{\Delta_0}, \quad (14)$$

and

$$S_{0,0} = \frac{1}{2\pi\Sigma_0 R_c}\int_0^{2\pi} \Sigma(\theta) a d\theta \quad (15)$$

called the 'surface factor' in the following. In this paper, we will consider *homogeneous* shells, so we set $\Sigma = \text{const.} = \Sigma_0$. Anticipating higher orders, let us define the whole series of definite integrals

$$J_{n,m} = \frac{1}{2\pi}\int_0^{2\pi} \cos^n\theta \sin^m\theta d\theta, \quad (16)$$

where n and m are positive integers. They can all be written in terms of the complete Beta function $B(\frac{n+1}{2}, \frac{m+1}{2})$; see Appendix A. We give $J_{n,m}$ for the first few values of n and m in Table 1. We note in particular that $J_{n,m} = 0$ when either m or n or $m+n$ is odd. We have $S_{0,0} = J_{0,0} + eJ_{1,0} = 1$ and so the zero-order approximation for the potential of the shell is approximately given by

$$\Psi_0(\vec{r}) = -8\pi G\Sigma_0 b R_c \kappa_0. \quad (17)$$

Table 1. Expressions for $J_{n,m}$ required when expanding the Green function up to second order. Also given are the surface factor $S_{n,m}$ and the volume factor $V_{n,m}$.

$n+m$	n	m	$J_{n,m}$	$S_{n,m}$	$V_{n,m}$
0	0	0	$\frac{1}{\pi}B(\frac{1}{2},\frac{1}{2})=1$	1	1
1	1	0	0	$\frac{1}{2}e^2$	$\frac{1}{4}e^2$
	0	1	0		
2	2	0	$\frac{1}{\pi}B(\frac{3}{2},\frac{1}{2})=\frac{1}{2}$	$\frac{1}{2}e^2$	$\frac{1}{4}e^2$
	1	1	0		
	0	2	$\frac{1}{\pi}B(\frac{1}{2},\frac{3}{2})=\frac{1}{2}$	$\frac{1}{2}e^2$	$\frac{1}{4}e^2$
3	3	0	0		
	2	1	0		
	1	2	0		

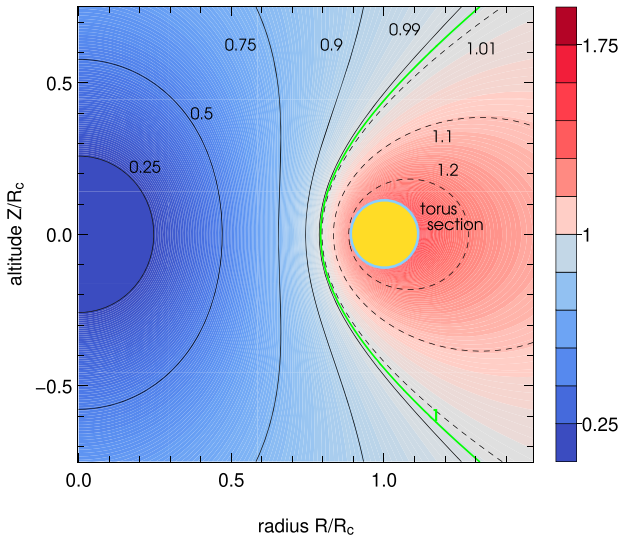

Figure 3. The factor $g_{0,0}$ given by equation (19) and representing the deviation between the potential of a monopole and the zero-order potential of the toroidal shell. The conditions are the same as for Fig. 2. The shell section is indicated (*thick black line*). A few contour lines are given: $g_{0,0}<1$ (*blue domain*), $g_{0,0}=1$ (*green line*), and $g_{0,0}>1$ (*red domain*).

3.1 Comparison with the potential of a point mass

It is easy to compare equation (17) to the potential of some simple sources, like the potential of a monopole (or point mass at the origin), which is of major interest in dynamical studies. Introducing the mass of the homogeneous shell $M_{\rm shell}=4\pi^2\Sigma_0 bR_c$, equation (17) writes

$$\Psi_0(\vec{r})=-\frac{GM_{\rm shell}}{r}\times g_{0,0}, \tag{18}$$

where $r=\sqrt{R^2+Z^2}$ is the spherical radius, and

$$g_{0,0}=\frac{r}{\Delta_0}\frac{2}{\pi}\mathbf{K}(k_0). \tag{19}$$

We see that equation (17) differs from the monopole potential only by the quantity $g_{0,0}$, which is a function of the position in space only. In the physical space, it also depends on R_c, but not on e, i.e. $g_{0,0}\equiv g_{0,0}(\vec{r};R_c)$. The meridional-plane contours of $g_{0,0}$ are shown in Fig. 3 in the neighbourhood of the shell. The contours are closed, except the $g_{0,0}=1$ one. The region where $g_{0,0}>1$ surrounds the shell section, while $g_{0,0}<1$ concerns the central region near the Z-axis. This kind of map is helpful for dynamical studies since it indicates very well the families of bounded and unbounded trajectories of test particles moving with a constant angular momentum (on equatorial or inclined toroidal orbits and on purely meridional orbits).

3.2 Comparison with the potential of a circular loop

Let us also compare the zero-order shell potential (equation 17) and that of a circular loop of radius R_c and mass $M_{\rm loop}=2\pi\lambda R_c$, which writes

$$\Psi^{\rm loop}(\vec{r})=-2G\lambda\sqrt{\frac{a}{R}}k_0\mathbf{K}(k_0)$$
$$=-\frac{GM_{\rm loop}}{r}\underbrace{\frac{r}{\Delta_0}\frac{2}{\pi}\mathbf{K}(k_0)}_{g_{0,0}}. \tag{20}$$

We see that, at the zeroth order, $\Psi_0=\Psi^{\rm loop}$ at any point P in space, and for any value of e, provided $M_{\rm shell}=M_{\rm loop}$. According to Kondratyev (2018) (see also below), there is no term in the expansion led by e and, more generally, by odd powers of e (this is not guaranteed as soon as Σ varies with θ). This implies that $\Psi^{\rm shell}=\Psi^{\rm loop}+\mathcal{O}(e^2)$. We can thus conclude (similarity theorem 1) that

a homogeneous toroidal shell of main radius R_c and circular section generates, at the first order in the e-parameter, the same exterior potential as a circular loop of same radius R_c and same mass.

This result has a few important consequences. First, the approximation thus behaves correctly at infinity and on the Z-axis as well ($\lim_{k\to0}\mathbf{K}(k_0)=\frac{\pi}{2}$ and $k_0/\sqrt{R}$ is finite at the Z-axis). Second, the gravitational acceleration inherits these properties, i.e. the similarity theorem also applies to $\vec{g}=-\nabla\Psi$ (see below). Third, the formula in equation (17) does not generate any residual mass distribution in space. This is easily verifiable by calculating the Laplacian of κ_0 (see Appendix B for the demonstration), i.e.

$$\nabla^2\Psi_0=4\pi G\rho^{\rm res}=0. \tag{21}$$

This property is also intrinsic to the interior solutions reported in Huré et al. (2019).

4 NUMERICAL TESTS. DOMAIN OF VALIDITY

Let us now compare the expression (equation 17) to the numerical reference (see Section 2). We quantify the relative difference by

$$\epsilon=\log\left|\frac{\Psi-\Psi_{\rm ref}}{\Psi_{\rm ref}}\right|. \tag{22}$$

Fig. 4 shows ϵ in the upper half-plane $Z>0$ for $e=0.1$. If we limit the statistics to the domain exterior to the shell, the average precision is of the order of 10^{-3} in the vicinity of the shell, and it is much lower in the far field. The deviation with respect to the reference never exceeds 1 per cent. The error is maximal near the surface of the shell, which is not a surprise. On the other hand, the best approximation is achieved in a narrow domain going from the top of the shell to infinity along the line $Z\sim0.7R$.

Our expansion is performed at the centre C of the shell section. The expanded function thus has to be smooth enough between C and any point P′ located at the shell surface. This, however, is not the

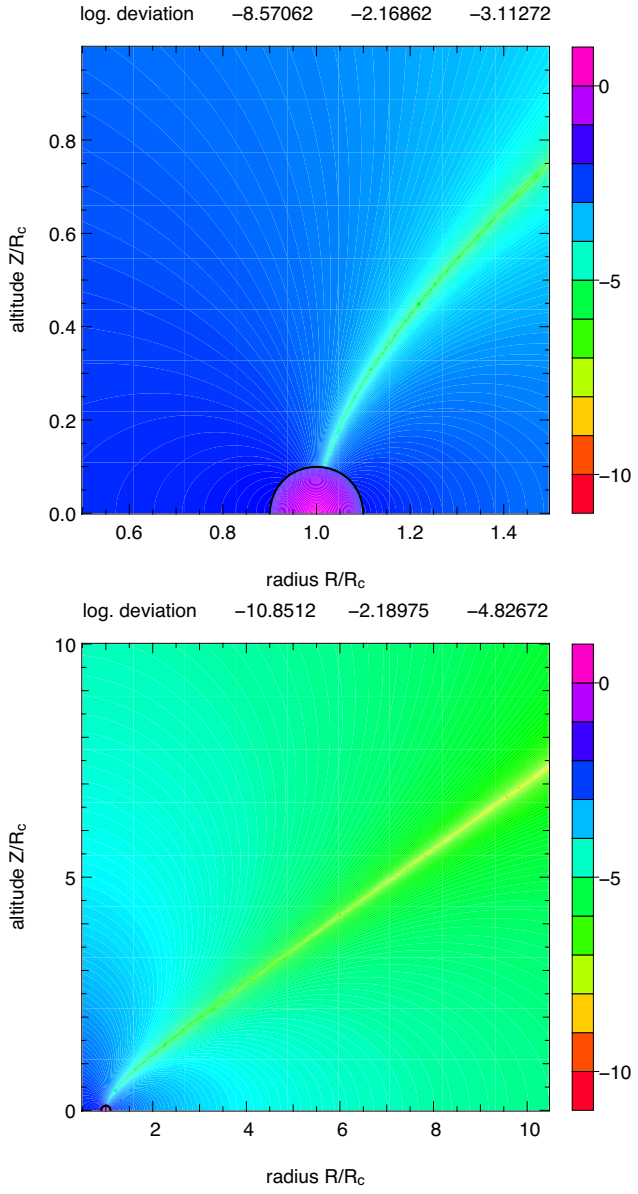

Figure 4. The log of the relative deviation defined by equation (22) between Ψ computed by direct integration, i.e. $\Psi_{\rm ref}$, and the zero-order approximation given by equation (17), in the vicinity of the shell (top) and at longer range (bottom). The parameter of the shell (thick black circle) is $e = 0.1$; see Fig. 2 for the associated potential. The numbers given at the top, from left to right, refer to the minimal, maximal, and mean values for ϵ, respectively, reached within the actual computational box (and exterior to the shell).

case for $\mathbf{K}(k)/\Delta$, which is singular for any point P(R, Z) belonging to the line segment [CP′]. Therefore, the formula in equation (10) and subsequently *the zero-order approximation is only valid outside the cavity*, namely for

$$(R - R_c)^2 + Z^2 - b^2 \; > \; 0. \tag{23}$$

The comparison has been checked for different values of the shell parameter e. The results are plotted in Fig. 5, where values of ϵ have been averaged over values contained inside a squared box $[1 - 2e, 1 + 2e] \times [0, 4e]$ (in dimensionless units) encompassing the shell section (see Fig. 4); interior values are excluded. We see that the smaller the shell parameter, the better the approximation.

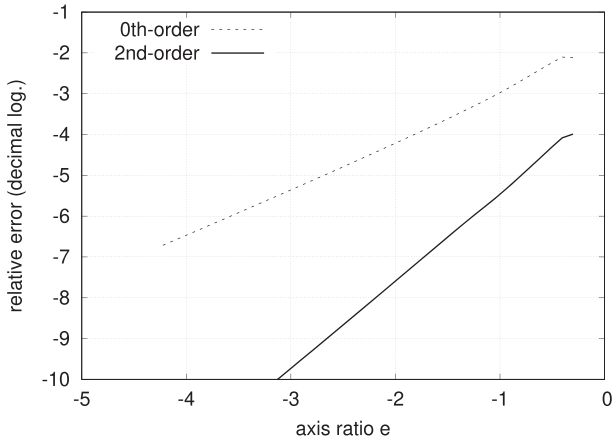

Figure 5. Average of the log of the relative deviation defined by equation (22) versus the shell parameter for the zeroth-order (dotted line) and the second-order approximation (solid line). The sample gathers values contained inside the computational box $4e \times 4e$ around the shell section (and exterior to it).

The precision of the zero-order approximation remains better than 1 per cent for shell parameter as large as about 0.3, which is remarkable.

5 EXPANSION UP TO SECOND ORDER

Though already very good, the zero-order approximation can be improved by considering further terms in the expansion. For order 1, we have to calculate

$$\int_0^{2\pi} \left[(a - R_c) \left.\frac{\partial \kappa}{\partial a}\right|_{\substack{a=R_c \\ z=0}} + z \left.\frac{\partial \kappa}{\partial z}\right|_{\substack{a=R_c \\ z=0}} \right] abd\theta, \tag{24}$$

where a and z are still given by equation (7). Because the derivatives are evaluated at $a = R_c$ and $z = 0$, they are not concerned by the integration over θ and can be carried out of the operator. There are two new surface factors to calculate, namely (we do not include Σ in these definitions, since we assume it is constant)

$$S_{1,0} = \frac{1}{2\pi R_c^2} \int_0^{2\pi} (a - R_c) a d\theta \tag{25}$$

and

$$S_{0,1} = \frac{1}{2\pi R_c^2} \int_0^{2\pi} z a d\theta, \tag{26}$$

but this latter term vanishes (since $J_{0,1}$ and $J_{1,1}$ are zero). In the first order, the potential writes $\Psi \approx \Psi_0 + \Psi_1$, where Ψ_0 is given by equation (17) and

$$\Psi_1 = -8\pi G \Sigma_0 b R_c^2 \left.\frac{\partial \kappa}{\partial a}\right|_{R_c,0} \times S_{1,0}, \tag{27}$$

where $S_{1,0} = e(J_{1,0} + eJ_{2,0})$. Note that the derivative $\frac{\partial \kappa}{\partial a}$ is analytical (see Appendix C). Since $J_{1,0} = 0$, the first-order correction depends on e^2. As $2\pi J_{2,0} = 2B(\frac{3}{2}, \frac{1}{2}) = \pi$, we have

$$S_{1,0} = \frac{1}{2} e^2. \tag{28}$$

It is pertinent to account for the next term in the Taylor expansion, which also contains a contribution varying as e^2. This term is

$$\frac{1}{2}\int_0^{2\pi}\left[(a-R_c)^2\left.\frac{\partial^2\kappa}{\partial a^2}\right|_{\substack{R_c\\0}}+2(a-R_c)z\left.\frac{\partial^2\kappa}{\partial a\partial z}\right|_{\substack{R_c\\0}}+z^2\left.\frac{\partial^2\kappa}{\partial z^2}\right|_{\substack{R_c\\0}}\right]abd\theta, \tag{29}$$

and so the second-order approximation is given by $\Psi \approx \Psi_0 + \Psi_1 + \Psi_2$, with

$$\Psi_2 = -8\pi G\Sigma_0 b R_c^3 \times\frac{1}{2}\left[\left.\frac{\partial^2\kappa}{\partial a^2}\right|_{\substack{R_c\\0}}S_{2,0}+2\left.\frac{\partial^2\kappa}{\partial a\partial z}\right|_{\substack{R_c\\0}}S_{1,1}+\left.\frac{\partial^2\kappa}{\partial z^2}\right|_{\substack{R_c\\0}}S_{0,2}\right], \tag{30}$$

where the derivatives are given in Appendix C. The new surface factors are (again, Σ is removed from these definitions)

$$S_{2,0}=\frac{1}{2\pi R_c^3}\int_0^{2\pi}(a-R_c)^2 a d\theta, \tag{31}$$

$$S_{1,1}=\frac{1}{2\pi R_c^3}\int_0^{2\pi}(a-R_c) z a d\theta, \tag{32}$$

and

$$S_{0,2}=\frac{1}{2\pi R_c^3}\int_0^{2\pi} z^2 a d\theta. \tag{33}$$

We see that $S_{1,1} = 0$, again because of the odd power of z. The non-zero terms are $S_{2,0} = e^2(J_{2,0} + eJ_{3,0})$ and $S_{0,2} = e^2(J_{0,2} + eJ_{1,2})$, where $J_{3,0} = J_{1,2} = 0$, $2\pi J_{2,0} = 2B(\frac{3}{2}, \frac{1}{2}) = \pi$. $S_{2,0} = S_{0,2} = \frac{1}{2}e^2$. We thus see that it is necessary to include *both* orders 1 and 2 simultaneously in order to obtain a consistent e^2-approximation. This new approximation can be put in the form of a modified monopole, like we did for the zeroth-order expression. There is one specific correction factor $g_{n,m} \equiv g_{n,m}(\vec{r}; R_c, e)$ for each non-zero surface factor $S_{n,m}$. We find

$$\Psi_1 = -\frac{GM_{\rm shell}}{r}g_{1,0}, \tag{34}$$

where

$$g_{1,0} = r\frac{2}{\pi}\left.\frac{\partial\kappa}{\partial a}\right|_{\substack{a=R_c\\z=0}}R_c S_{1,0}, \tag{35}$$

and

$$\Psi_2 = -\frac{GM_{\rm shell}}{r}\frac{1}{2}\left(g_{2,0}+g_{0,2}\right), \tag{36}$$

where

$$g_{2,0} = r\frac{2}{\pi}\left.\frac{\partial^2\kappa}{\partial a^2}\right|_{\substack{a=R_c\\z=0}}R_c^2 S_{2,0}, \tag{37}$$

and

$$g_{0,2} = r\frac{2}{\pi}\left.\frac{\partial^2\kappa}{\partial z^2}\right|_{\substack{a=R_c\\z=0}}R_c^2 S_{0,2}. \tag{38}$$

Because of the circular section, $S_{2,0} = S_{0,2}$, which implies that the partial sum $\Psi_1 + \Psi_2$ can be rewritten in a very compact form.

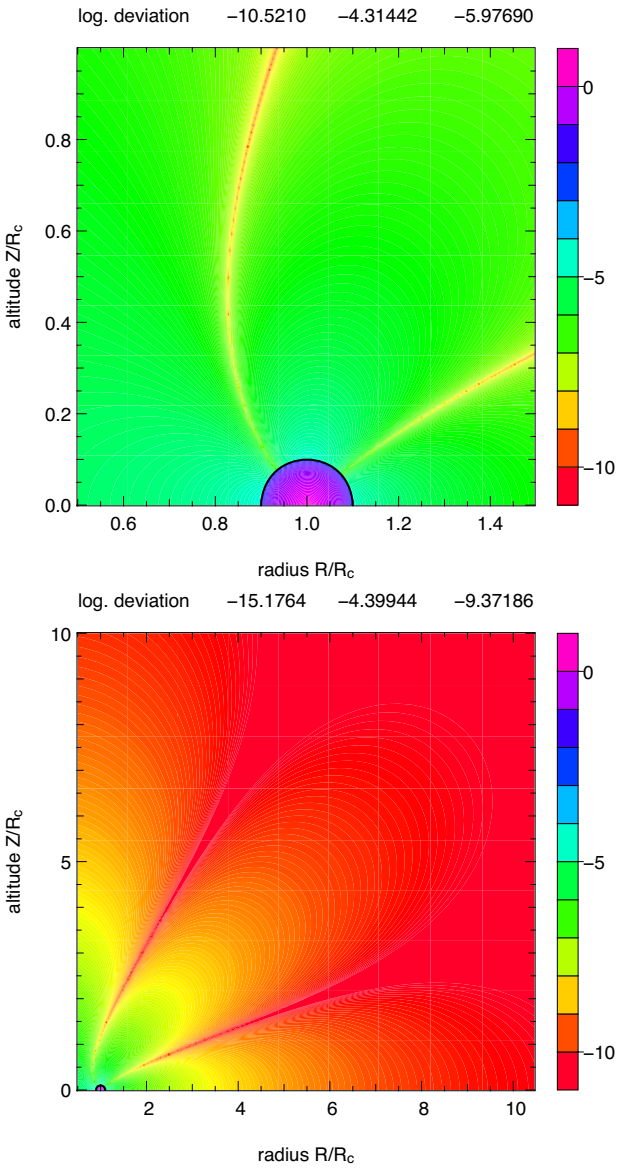

Figure 6. The same legend and the same conditions as for Fig. 4, but for the second-order approximation (i.e. e^2-approximation).

We actually find

$$g_{1,0}+\frac{1}{2}\left(g_{2,0}+g_{0,2}\right) = r\frac{2}{\pi}\times\frac{e^2}{8k'^2\Delta_0^3} \times\left\{\left[\Delta_0^2-2R_c(R_c+R)\right]\mathbf{E}(k)-k'^2\Delta_0^2\mathbf{K}(k)\right\}, \tag{39}$$

which is to be multiplied by $-GM_{\rm shell}/r$.

Fig. 6 compares the second-order approximation obtained from equations (17), (27), and (30) with the reference values (see Section 2), as computed under the same conditions as in Fig. 4. We notice that the e^2-approximation reproduces the potential with almost six-digit precision in the close vicinity of the shell. At larger distances, the expansion is extremely efficient (in the present example, the potential is known with more than 10 digits for $r/R_c \gtrsim 5$ typically). The variation of the averaged precision as a function of the shell parameter e is plotted in Fig. 5, in the same conditions as for the zeroth-order approximation.

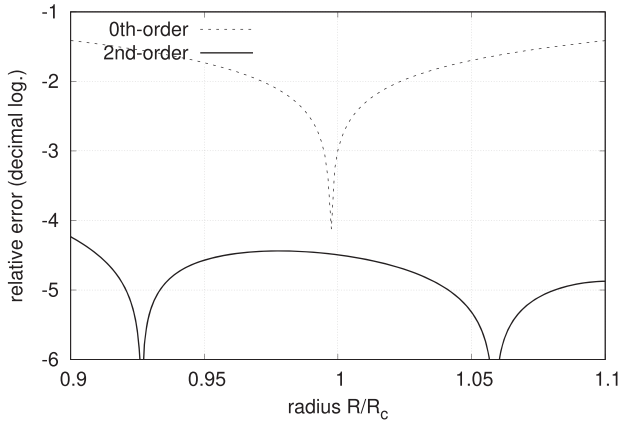

Figure 7. Logarithm of the difference between the interior solution (Huré et al. 2019) and the exterior solution for the zeroth-order (dotted line) and second-order approximations (plain line). The shell parameter is $e = 0.1$.

6 VALUES AT THE SURFACE. MATCH WITH THE INTERIOR SOLUTION

At the surface of the shell, we have $R = R_c + b\cos\theta$ and $Z = b\sin\theta$, or equivalently $(R - R_c)^2 + Z^2 - b^2 = 0$ with $R \in [R_c - b, R_c + b]$. If we introduce these expressions in equation (12), the modulus k_0 simplifies into

$$k_0{}^2 = \frac{4RR_c}{4RR_c + b^2}. \tag{40}$$

Using these values in equations (17), (27), and (30), we get the potential at the shell surface, which can be compared to the values obtained from the interior solution reported in Huré et al. (2019); see their equations (35), (36), and (39). The results are displayed in Fig. 7, again for $e = 0.1$. We see that the matching is very good at the second order (with at least four correct digits). At the zeroth order, the interior solution reduces to a constant potential throughout the toroidal cavity, which is quite crude while the exterior solution already depends on the radius R.

7 GENERALIZATION TO *N*TH-ORDER EXPANSION

It is possible to include further terms in the Taylor series. Since the expansion writes formally

$$\kappa = \kappa_0 + \sum_{n=1}^{\infty} \frac{1}{n!} \sum_{m=0}^{n} \binom{n}{m} (a - R_c)^{n-m} z^m \times \left. \frac{\partial^n \kappa}{\partial a^{n-m} \partial z^m} \right|_{\substack{a=R_c \\ z=0}}, \tag{41}$$

where $\binom{n}{m}$ denotes the binomial coefficient, the potential can be exactly reconstructed by multiplying equation (41) by a, followed by the integration over the latitude angle θ. If the infinite series is truncated at order N, the potential is of the form

$$\Psi \approx \Psi_0 + \sum_{n=1}^{N} \Psi_n, \tag{42}$$

where the nth-order contribution Ψ_n is made of $n + 1$ terms, namely

$$\Psi_n = -4G\Sigma_0 \frac{1}{n!} \sum_{m=0}^{n} \binom{n}{m} \times \left. \frac{\partial^n \kappa}{\partial a^{n-m} \partial z^m} \right|_{\substack{a=R_c \\ z=0}} \times 2\pi b R_c^{n+1} S_{n-m,m}, \tag{43}$$

where we have set (still in the homogeneous case)

$$S_{n,m} = \frac{1}{2\pi R_c^{n+m+1}} \int_0^{2\pi} (a - R_c)^n z^m a d\theta = e^{n+m}(J_{n,m} + eJ_{n+1,m}). \tag{44}$$

Note that $\Psi_{n+1} \ll \Psi_n$ when $e \ll 1$, and the equality in equation (42) is obtained in the limit $N \to \infty$. In the form of the modified monopole representation, the n-order correction is

$$\Psi_n = -\frac{GM_{\rm shell}}{r} \sum_{m=0}^{n} g_{n,m}, \tag{45}$$

where

$$g_{n,m} = \frac{2}{\pi} r \times \frac{1}{n!} \binom{n}{m} \left. \frac{\partial^n \kappa}{\partial a^{n-m} \partial z^m} \right|_{\substack{a=R_c \\ z=0}} R_c^n S_{n-m,m}. \tag{46}$$

Since the two operators $\nabla^2_{R,Z}$ and $\partial^n / \partial a^{n-m} \partial z^m$ act on different spaces, we have

$$\nabla^2_{R,Z} \left(\frac{\partial^n \kappa}{\partial a^{n-m} \partial z^m} \right) = \frac{\partial^n}{\partial a^{n-m} \partial z^m} \left(\nabla^2_{R,Z} \kappa \right) = 0 \tag{47}$$

for any pair (n, m). This is expected because κ is a harmonic function (see Section 4). We thus conclude that $\nabla^2_{R,Z} \Psi_n = 0$, for any n, which means that each term of the expansion separately obeys the Laplace equation. Therefore, expanding the Green function over a and z induces no residual source mass in space, whatever the order of the truncation.

8 THE SOLID TORUS

The above solution for the shell can be employed to obtain the potential of a solid toroid. This is achieved by integrating equation (6) over b, while the surface density Σ is changed for ρdb, ρ being the mass density. The result is

$$\Psi(\vec{r}) = -4G \int_0^b \int_0^{2\pi} \rho(b', \theta) a \kappa b' d\theta db', \tag{48}$$

where κ can be replaced by its Taylor expansion, namely equation (10). In the leading term, i.e. using just equation (17), we have

$$\Psi_0(\vec{r}) = -4G\kappa_0 \times \pi R_c b^2 \rho_0 V_{0,0}, \tag{49}$$

where ρ_0 is some typical mass density, and $V_{0,0}$ is the 'volume factor' defined in general by

$$V_{0,0} = \frac{1}{\pi \rho_0 R_c b^2} \int_0^b b' db' \int_0^{2\pi} \rho(b', \theta) a d\theta, \tag{50}$$

where $b' = e' R_c \leq b$. As quoted, the mass density ρ may vary with both θ and b' (see below). In the *homogeneous case*, we have $\rho = \text{const.} = \rho_0$, and so equation (50) becomes

$$V_{0,0} = \frac{2}{\rho_0 e^2} \int_0^e \rho(e') e' S_{0,0}(e') de' = \frac{2}{e^2} \int_0^e e' S_{0,0}(e') de', \tag{51}$$

Table 2. Expressions for the volume factor $V_{n,m}$ in the case of core-stratified toroids according to equations (58) and (59).

$n+m$	n	m	$V_{n,m}$ homogeneous	Equation (59)
0	0	0	1	$\frac{\alpha}{\alpha+1}$
1	1	0	$\frac{1}{4}e^2$	$\frac{\alpha}{4(\alpha+2)}e^2$
	0	1		
2	2	0	$\frac{1}{4}e^2$	$\frac{\alpha}{4(\alpha+2)}e^2$
	1	1	0	0
	0	2	$\frac{1}{4}e^2$	$\frac{\alpha}{4(\alpha+2)}e^2$

where the dependence of the surface factor with the shell parameter e has been explicit. Introducing the total mass of the homogeneous torus $M_{\rm solid} = 2\pi^2\rho_0 b^2 R_c$, the zero-order formula can be written in the form

$$\Psi_0(\vec{r}) = -\frac{GM_{\rm solid}}{r} g_{0,0}, \tag{52}$$

where we have set

$$g_{0,0} = \frac{r}{\Delta_0}\frac{2}{\pi}\mathbf{K}(k_0)V_{0,0}. \tag{53}$$

Again, the difference from the point-mass potential is represented by the term $g_{0,0}$, while the deviation with respect to the potential of a massive loop (of radius $a = R_c$) is given by the volume factor $V_{0,0}$. For the zero-order approximation, we have $V_{0,0} = 1$, and so $\Psi^{\rm solid} = \Psi^{\rm loop} + \mathcal{O}(e^2)$. We can thus conclude (similarity theorem 2) that

a solid torus of main radius R_c and circular section generates, at the first order in the e-parameter, the same exterior potential as a circular loop of radius R_c and same mass.

The derivation of the e^2-term requires $V_{1,0}$, $V_{2,0}$, and $V_{0,2}$, which are listed in Table 2. These quantities happen to be equal (due to the circular section). As a consequence, the partial sum $\Psi_1 + \Psi_2$ resembles[1] the formula derived in Kondratyev (2018). We finally find

$$\Psi_1 + \Psi_2 = e^2\left(-\frac{G\pi\rho_0 R_c b^2}{4k'^2\Delta_0^3}\left\{\left[\Delta_0^2 - 2R_c(R_c+R)\right]\mathbf{E}(k) - k'^2\Delta_0^2\mathbf{K}(k)\right\}\right). \tag{54}$$

We have compared equation (49) to a reference obtained by direct numerical integration of equation (48). As we have observed, the error map is the same as for the shell, which is expected since the only difference between the shell and the torus stands in the volume factor that is analytical. This remark holds for the e^2-approximation.

More terms in the expansion of κ can be accounted for. The n-order contribution is

$$\Psi_n = -4G\frac{1}{n!}\sum_{m=0}^{n}\binom{n}{m}\left.\frac{\partial^n\kappa}{\partial a^{n-m}\partial z^m}\right|_{\substack{a=R_c\\z=0}} \times 2\pi R_c^{n+1}\rho_0\int_0^b S_{n-m,m}(b')b'db', \tag{55}$$

[1]We notice two differences between equation (54) and the formula (14) by Kondratyev (2018): the factor R_0^3 should be $R_0 r_0^2 \equiv R_c b^2$ (since the ϕ_2 term is multiplied by e^2), and the factor 16 at the denominator should be 4.

where $S_{n-m,m}$ depends on b' as indicated. If we set the volume factor $V_{n,m}$ to

$$V_{n,m} = \frac{1}{2\pi R_c^{n+m+1}}\frac{2}{b^2}\int_0^b b'db'\int_0^{2\pi}(a-R_c)^n z^m a d\theta = \frac{2}{e^2}\int_0^e S_{n,m}(e')e'de', \tag{56}$$

then Ψ_n has the same form as equation (45), where $S_{n-m,m}$ is just to be replaced by $V_{n-m,m}$ and $M_{\rm shell}$ by $M_{\rm solid}$. It can be checked that Ψ_n is harmonic.

9 INHOMOGENEOUS SYSTEMS

As a matter of fact, equation (41) works for inhomogeneous systems. Actually, the expansion depends on a and z only through powers of $\cos\theta$ and $\sin\theta$. If $\Sigma(\theta)$ is prescribed, the knowledge of any term Ψ_n just requires the calculation of the surface factors according to

$$S_{n,m} = \frac{1}{2\pi\Sigma_0 R_c^{n+m+1}}\int_0^{2\pi}\Sigma(\theta)(a-R_c)^n z^m a d\theta = \frac{e^{m+n}}{2\pi\Sigma_0}\int_0^{2\pi}\Sigma(\theta)\cos^n\theta\sin^m\theta(1+e\cos\theta)d\theta. \tag{57}$$

We see that the $S_{n,m}$s are combinations of moments of the surface density profile, which are analytical for a wide family of $\Sigma(\theta)$ profiles. In a similar way for the solid torus, if ρ depends both on θ and $b' \le b$, then the volume factors are calculated following

$$V_{n,m} = \frac{1}{2\pi\rho_0 R_c^{n+m+1}}\frac{2}{b^2}\int_0^b b'db'\int_0^{2\pi}\rho(b',\theta)(a-R_c)^n z^m a d\theta = \frac{e^{m+n}}{\pi\rho_0}\int_0^1 x'^{n+m+1}dx' \times\int_0^{2\pi}\rho(x',\theta)\cos^n\theta\sin^m\theta(1+bx'\cos\theta)d\theta, \tag{58}$$

where we have set $b' = bx' \le b$. We can go a little bit further in the analysis by considering the case where the two variables b' and θ are separable, i.e. $\rho(b',\theta) = f(b')\times g(\theta)$. This corresponds to toroids having a core stratification. For instance, if we assume the θ invariance and (with $2\alpha > -1$)

$$\rho(b') = \rho_0\left[1-\left(\frac{b'}{b}\right)^{2\alpha}\right], \tag{59}$$

then the volume factor required at order zero (i.e. $n = m = 0$) is

$$V_{0,0} = \int_0^1 2x'(1-x'^{2\alpha})dx' = \frac{\alpha}{1+\alpha}. \tag{60}$$

Note that $V_{0,0} \to 1$ as $\alpha \to \infty$. Since $M_{\rm solid}V_{0,0}$ is just the total mass M of the (inhomogeneous) core-stratified torus, we have $\Psi = \Psi^{\rm loop} + \mathcal{O}(e^2)$. We can conclude (similarity theorem 3) that

a core-stratified torus of main radius R_c and circular section generates, at the first order in the e-parameter, the same exterior potential as a circular loop of radius R_c and same mass.

Table 2 lists values of $V_{n,m}$ corresponding to equation (59).

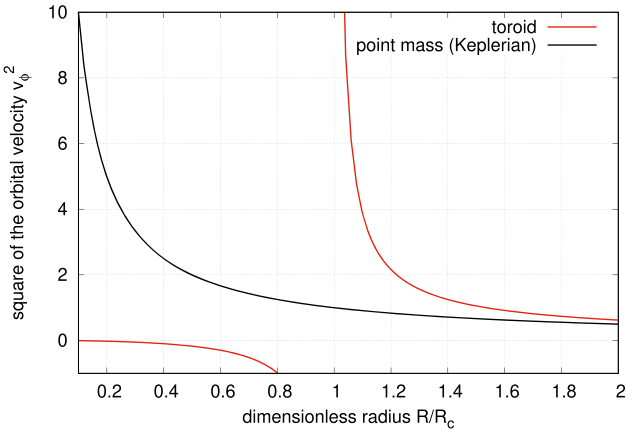

Figure 8. Square of the circular velocity in the equatorial plane of the toroid as given by equation (63), i.e. at order zero. The curve has to be truncated at the actual outer radius, which is $1 + e$ in dimensionless units. Negative values take sense only when a massive central object is present. The Keplerian velocity due to a point mass with the same mass is shown in comparison.

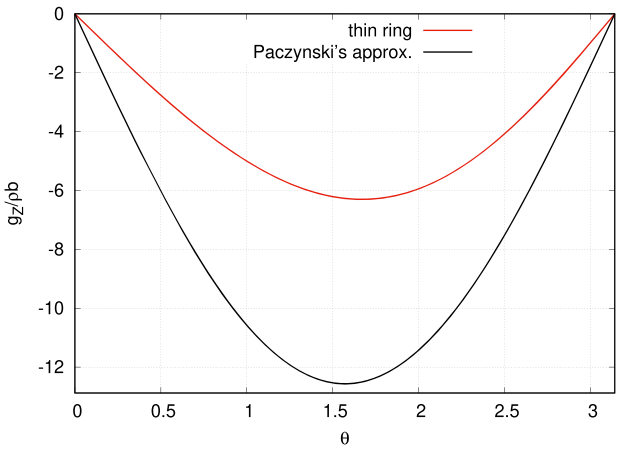

Figure 9. Vertical acceleration at the surface of the toroid in units of $G\rho b$. Paczynski's approximation valid for geometrically thin, extended systems is shown in comparison.

10 GRAVITATIONAL ACCELERATION

For a massive loop, the non-zero components of acceleration $\vec{g} = -\vec{\nabla}\Psi$ are given by (Durand 1953; Huré 2005)

$$g_R = \frac{GM_{\rm loop}}{2\pi R_c R}\sqrt{\frac{R_c}{R}} \times k_0\left[\mathbf{E}(k_0) - \mathbf{K}(k_0) + \frac{(R_c - R){k_0}^2\mathbf{E}(k_0)}{2R_c {k_0'}^2}\right], \quad (61)$$

and

$$g_Z = -\frac{GM_{\rm loop}Z}{4\pi R R_c\sqrt{RR_c}}\frac{{k_0}^3\mathbf{E}(k_0)}{{k_0'}^2}. \quad (62)$$

According to the similarity theorems 1 to 3, the acceleration outside a shell, solid torus, or core-stratified toroid is the same as for a loop having the same mass M, and deviations are $\mathcal{O}(e^2)$. This result is very convenient for a study of the motion of orbiting test particles. Several types of trajectories can be distinguished. Of particular interest are circular trajectories tied to the equatorial plane of the shell/torus and having $R \notin [R_c - b, R_c + b]$. The orbital velocity $v_\phi^2 = R\nabla_R\Psi$ is easily deduced from equation (61). We find

$$v_\phi^2(R) = \frac{GM}{R + R_c}\frac{1}{\pi}\left[\mathbf{K}(k_0) + \frac{R + R_c}{R - R_c}\mathbf{E}(k_0)\right], \quad (63)$$

where $k_0 = \frac{2\sqrt{RR_c}}{R+R_c}$ follows from equation (12), where Z has been set to 0. Fig. 8 displays equation (63) versus the radius. Note that $v_\phi^2(R) \leq 0$ for $R \in [0, R_c - b]$, which means that orbits are in principle forbidden in this region, unless a massive central object is present. The Keplerian profile associated to a point mass at the origin is shown in comparison. For $R \geq R_c + b$, the velocity is super-Keplerian. It is a decreasing function of the radius, the maximum value being reached at the outer radius $R_c + b$ of the toroid. To the detriment of precision, we can replace the elliptic integrals by more standard functions when $k_0 \to 1$, which corresponds to particles orbiting very close to the inner/outer radius of the toroid. Within this limit, $\mathbf{K}(k_0) \sim \ln\frac{4(R+R_c)}{|R-R_c|}$ and $\mathbf{E}(k_0) \sim 1$.

Another interesting quantity is the vertical component of acceleration at the surface of thin/small rings. It is a fundamental ingredient that governs the hydrostatic equilibrium of astrophysical discs (e.g. Shakura & Sunyaev 1973; Pringle 1981). By setting $\mathbf{E}(k_0) \approx 1$, which again corresponds to the vicinity of the toroid, we find

$$g_Z = -2\pi G\rho b\frac{\sin\theta}{\sqrt{1 + e\cos\theta + \frac{e^2}{4}}}, \quad (64)$$

where $\theta \in [0, \pi]$ above the equatorial plane. This quantity is plotted in Fig. 9 for $e = 0.1$ as the torus parameter. It varies between 0 at the inner/outer edges to about $-2\pi G\rho b$ at $\theta = \frac{\pi}{2}$. It is interesting to see that Paczynski's approximation (Paczynski 1978), classically written as $-4\pi G\rho Z$, overestimates the acceleration by a factor 2 in the middle of the toroid. This observation may be of importance in oscillation modes in planetary or other rings (Wisdom & Tremaine 1988; Lehmann et al. 2019). It also means that, in a geometrically thin discs where Paczynski's approximation is valid, half of the vertical acceleration comes from the local contribution of matter, while the other half comes from the global or long-range distribution of matter (Trova, Huré & Hersant 2014).

11 MAGNETIC POTENTIAL AND FIELD FOR PURELY AZIMUTHAL CURRENTS (IN SURFACE AND VOLUME)

The method presented in this paper can also be applied to the determination of the vector potential of electromagnetism. Toroidal currents are met in both terrestrial and astrophysical plasmas (Dini et al. 2009; Trova et al. 2018). The magnetic potential $\boldsymbol{A} = A_\phi\boldsymbol{e}_\phi$ of a toroidal shell carrying a purely azimuthal electric current $\sigma\vec{e}_\phi$ is obtained by summing over the contribution of individual current loops (Jackson 1998; Cohl et al. 2001), namely

$$A_\phi(\vec{r}) = \frac{\mu_0}{2\pi}\int_0^{2\pi}\sigma(\theta)\sqrt{\frac{a}{R}}\frac{(2 - k^2)\mathbf{K}(k) - 2\mathbf{E}(k)}{k}bd\theta, \quad (65)$$

where $I = b\oint\sigma(\theta)d\theta$ is the total current. Similarly as for the gravitational problem, we have to select some part of the Green function. A convenient choice appears to be

$$\frac{1}{\Delta}\left\{\frac{2}{k^2}\left[\mathbf{K}(k) - \mathbf{E}(k)\right] - \mathbf{K}(k)\right\} \equiv \kappa'. \quad (66)$$

By expanding κ' over a and z at the centre C of the shell, i.e. at $a = R_c$ and $z = 0$, and integrating over the latitude θ (see Section 3), we

get the leading term

$$A_\phi(\vec{r}) = \frac{\mu_0 b}{\pi} \times \kappa_0' \int_0^{2\pi} \sigma a d\theta = 2\mu_0 \sigma b R_c \kappa_0' S_{0,0}, \quad (67)$$

where κ_0' stands for κ' evaluated at C, σ = const. is assumed, and $S_{0,0}$ is given by equation (15). A θ-dependent surface density of current would lead to a different surface factor. Again, we notice that equation (67) formally differs from the expression for a current loop only by the term $S_{0,0}$, which is unity in the homogeneous case. We thus state (similarity theorem 4) that

a toroidal shell of main radius R_c and circular section carrying a uniform surface current generates, at the first order in the e-parameter, the same exterior magnetic potential as a circular loop of radius R_c carrying the same current.

The theorem holds in the $\mathcal{O}(e^2)$ order. It applies likewise to the magnetic field $\boldsymbol{B} = \nabla \times \boldsymbol{A}$. The e^2-approximations for the poloidal components B_R and B_Z of the shell are then given by

$$B_R = \frac{\mu_0 I}{2\pi} \frac{Z}{R\Delta_0} \left[\frac{R^2 + R_c^2 + Z^2}{(R - R_c)^2 + Z^2} \mathbf{E}(k_0) - \mathbf{K}(k_0) \right], \quad (68)$$

$$B_Z = \frac{\mu_0 I}{2\pi} \frac{1}{\Delta_0} \left[-\frac{R^2 - R_c^2 + Z^2}{(R - R_c)^2 + Z^2} \mathbf{E}(k_0) + \mathbf{K}(k_0) \right]. \quad (69)$$

We can deduce the magnetic potential and field of a solid torus carrying a uniform current density $\boldsymbol{J} = J_\phi \boldsymbol{e}_\phi$, following the procedure given in Section 8. The e^2-approximation for the vector potential is obtained from equation (67), where $S_{0,0}$ is to be replaced by $V_{0,0}$ (which is also unity in the present case). So, we can state (similarity theorem 5) that

a toroid of main radius R_c and circular section carrying a uniform volume current density generates, at the first order in the e-parameter, the same exterior magnetic potential (and the field) as a circular loop of radius R_c carrying the same current.

The reader can verify that this theorem also works for a core-stratified current, as for the gravitational problem.

12 GENERAL COMMENTS

The paper resides on the expansion of $\mathbf{K}(k)/\Delta$. Other options are possible as quoted before. If we expand $k\mathbf{K}(k)$ instead of $\mathbf{K}(k)/\Delta$ in the Green function, it can be shown that $g_{0,0}$ is changed for

$$g_{0,0} = \frac{r}{\Delta_0} \frac{2}{\pi} \mathbf{K}(k_0) \times S_{0,0}, \quad (70)$$

where

$$S_{0,0} = \frac{2}{\pi} \mathbf{E}(p) \sqrt{1+e}, \quad (71)$$

$$\mathbf{E}(k) = \int_0^{\pi/2} \sqrt{1 - k^2 \sin^2 \vartheta}\, d\vartheta \quad (72)$$

is the complete elliptic integral of the second kind, and

$$p^2 = \frac{2e}{1+e} \in [0, 1]. \quad (73)$$

With this approach, again, $S_{0,0}$ still does not depend on R and Z, but solely on e. It is plotted in Fig. 10. As we can see, its range of variation, namely $[\frac{2\sqrt{2}}{\pi}, 1]$, is very small. As a consequence, equations (19) and (70) are very close, and Fig. 3 is almost unchanged. Besides, we have

$$S_{0,0} = 1 - \frac{e^2}{16} - \frac{15e^4}{1024} + \ldots \quad (74)$$

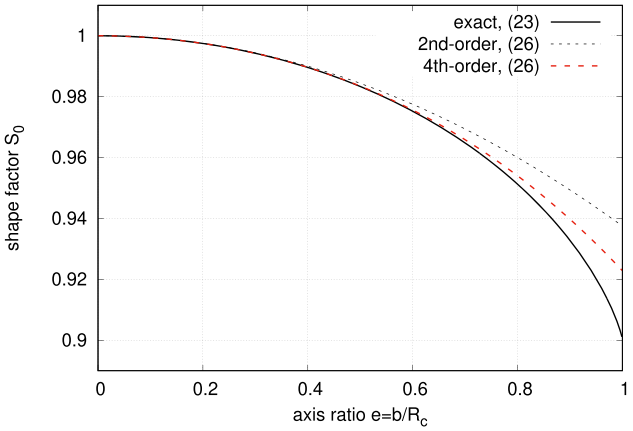

Figure 10. The quantity $S_{0,0}$ given by equation (71).

for $e \leq 1$. Since $S_{0,0} = 1$ for $e = 0$, we still have $\lim_{e \to 0} \Psi_0 = \Psi^{\rm loop}$.

The similarity theorem 1 reads in this case as

a homogeneous toroidal shell of mass M, main radius R_c, and circular section of radius $b = eR_c$ generates, at the second order in the e-parameter, the same exterior potential as a circular loop of radius R_c and mass $MS_{0,0}$, where $S_{0,0}$ is given by equation (71).

It can be shown after some algebra that the next three surface factors are respectively

$$S_{1,0} = \frac{2}{3\pi} \sqrt{1+e} \left[\mathbf{E}(p) - (1-e)\mathbf{K}(p) \right], \quad (75)$$

$$S_{2,0} = \frac{8}{15\pi} \sqrt{1+e} \left[\left(\frac{9}{2} e^2 - 1 \right) \mathbf{E}(p) + (1-e)\mathbf{K}(p) \right], \quad (76)$$

and

$$S_{0,2} = \frac{4}{15\pi} \sqrt{1+e} \left[(3e^2 + 1)\mathbf{E}(p) - (1-e)\mathbf{K}(p) \right], \quad (77)$$

and the corresponding error map is, as verified, similar to Fig. 6.

Another important comment concerns the point where the expansion is performed. In Huré et al. (2019), the choice for the expansion at the focal ring $a = R_{\rm p}$ was strategical: this is the only point in space that makes the modulus k of the elliptic integral constant all along the circular section of the shell. The motivation for choosing the centre of the circular section here (instead of the focal ring) is similar: the calculation of the integral in equation (6) is facilitated, in particular through the expression for $d\ell = bd\theta$. If we use for instance the toroidal coordinates $(\eta, \zeta) \in [0, \infty] \times [-\pi, \pi]$, the integral over θ in equation (6) can be converted into an integral over ζ. We have in this case

$$a = R_{\rm p} \frac{\sinh \eta}{\cosh \eta - \cos \zeta}, \qquad z = R_{\rm p} \frac{\sin \zeta}{\cosh \eta - \cos \zeta}, \quad (78)$$

where $R_{\rm p}$ is the radius of the pole (or focal ring), and the line element is $d\ell = R_{\rm p} \frac{d\zeta}{\cosh \eta - \cos \zeta}$. As a consequence, the potential writes

$$\Psi(\vec{r}) = -4G {R_{\rm p}}^2 \int_{-\pi}^{\pi} \frac{\mathbf{K}(k)}{\Delta} \sinh \eta \frac{\Sigma(\zeta) d\zeta}{(\cosh \eta - \cos \zeta)^2}, \quad (79)$$

where the modulus k and Δ depend on ζ. The expansion of κ in $x_0 = R_{\rm p}$ (and $y_0 = 0$ still; see Sections 3 and 7) generates, for the homogeneous shell, integrals of the form

$${R_{\rm p}}^{n+m+2} \int \frac{(\cosh \eta - \cos \zeta - \sinh \eta)^n}{(\cosh \eta - \cos \zeta)^{n+m+2}} \sin^m \zeta d\zeta. \quad (80)$$

At order zero (i.e. for $n = m = 0$), we find

$$\Psi(\vec{r}) \approx -8G {R_{\rm p}}^2 \Sigma_0 \kappa_0 S_{0,0}, \quad (81)$$

where

$$S_{0,0} = 2\sinh\eta_0 \int_{-\pi}^{\pi} \frac{d\zeta}{(\cosh\eta_0 - \cos\zeta)^2} = \frac{\cosh\eta_0}{\sinh^2\eta_0} = \frac{bR_c}{{R_\mathrm{p}}^2}, \quad (82)$$

and so we recover equation (17). For higher terms, (80) have to be calculated analytically for all pairs (n, m), and this manifestly requires more effort than for the J_{nm}s.

13 CONCLUSION AND PERSPECTIVES

The exterior potential of a static thin toroidal shell, as given by the Laplace equation, is obtained from a double Taylor expansion of the axisymmetric Green function. Each term is then integrated over the source, as in the multipole theory. Here, the expansion is performed at the centre of the circular section instead of the origin of coordinates. The series converges very well and provides a solution that satisfies the Laplace equation in every order, so no 'ghost' sources are induced by truncation. In practice, the efficiency of the method is remarkable, with already three correct digits at order zero for toroids having an axial ratio of 0.1. At order 2, this precision is almost doubled (to six digits), which should be sufficient for most applications.

At order 2 in the shell parameter (minor-to-major radius ratio), a shellular, solid, or core-stratified toroid generates an *exterior* potential (and field) similar to that of a thin circular loop having same main radius and same mass. We meet the results by Bannikova et al. (2011) and Kondratyev (2018). A few similarity theorems, which all resemble the Gauss theorem, have been proposed. The approximations for the exterior potential reported here together with the interior solutions reported in Huré et al. (2019) yield a complete description of the potential of a toroidal shell of circular section, at any point of space. It then becomes possible to deduce the interior solution for the solid torus, since both interior and exterior shell solutions are required in this operation. Next, the energy for the formation of a solid torus becomes accessible. It would be worth to generalize the method to any kind of source shape, not limited to circular section, through specific prescriptions for $a(\theta)$ and $z(\theta)$, or $z(a)$. This would open exciting perspectives, in particular for oblate structures such as geometrically thin discs.

ACKNOWLEDGEMENTS

We are grateful to the referee, Dr M. Majic, for useful comments, and in particular for pointing out the article by Kondratyev (2018) that we were not aware of at the time of submission.

V. Karas acknowledges Czech Science Foundation project no. 19-01137J. A. Trova acknowledges support from the Research Training Group 1620 'Models of Gravity' funded by the German Science Foundation DFG. O. Semerák is grateful for support from GACR-17/13525S grant of the Czech Science Foundation. We thank V. Tikhonchuk for references about terrestrial> plasmas.

REFERENCES

Abramowitz M., Stegun I. A., 1964, Handbook of Mathematical Functions with Formulas, Graphs, and Mathematical Tables. Dover, New York
Bannikova E. Y., Vakulik V. G., Shulga V. M., 2011, MNRAS, 411, 557
Binney J., Tremaine S., 1987, Galactic Dynamics. Princeton Univ. Press, Princeton, NJ, p. 747
Chandrasekhar S., 1987, Ellipsoidal Figures of Equilibrium, Dover, New York
Christodoulou D. M., 1993, ApJ, 412, 696
Clement M. J., 1974, ApJ, 194, 709
Cohl H. S., Rau A. R. P., Tohline J. E., Browne D. A., Cazes J. E., Barnes E. I., 2001, Phys. Rev. A, 64, 052509
Dini F., Baghdadi R., Amrollahi R., Khorasani S., 2009, preprint (arXiv: 0909.0660)
Durand E., 1953, Electrostatique et Magnetostatique. Masson & Cie, Paris
Dyson F. W., 1893, Phil. Trans. R. Soc. A, 184, 1041
Eriguchi Y., Mueller E., 1993, ApJ, 416, 666
Fukushima T., 2016, MNRAS, 463, 1500
Gradshteyn I. S., Ryzhik I. M., 2007, Table of Integrals, Series, and Products, 7th edn. Academic Press, Amsterdam
Guilloteau S., Dutrey A., Simon M., 1999, A&A, 348, 570
Hachisu I., 1986, ApJS, 61, 479
Hashimoto M., Eriguchi Y., Arai K., Mueller E., 1993, A&A, 268, 131
Horedt G. P., ed., 2004, Polytropes - Applications in Astrophysics and Related Fields. Kluwer Academic Publishers, Dordrecht
Huré J.-M., 2005, A&A, 434, 1
Huré J., Trova A., Karas V., Lesca C., 2019, MNRAS, 486, 5656
Iorio L., 2012, Earth Moon Planets, 108, 189
Jackson J. D., 1998, Classical Electrodynamics, 3rd edn. Wiley-VCH, Hoboken, NJ
Kellogg O. D., 1929, Foundations of Potential Theory. Frederick Ungar Publishing Company, New York
Kondratyev B. P., 2018, Tech. Phys., 63, 311
Lehmann M., Schmidt J., Salo H., 2019, A&A, 623, A121
Majic M., 2020, Appl. Numer. Math., 148, 98
Nieto M. M., 2005, Phys. Rev. D, 72, 083004
Nishida S., Eriguchi Y., 1994, ApJ, 427, 429
Paczynski B., 1978, Acta Astron., 28, 91
Petroff D., Horatschek S., 2008, MNRAS, 389, 156
Pickett B. K., Durisen R. H., Link R., 1997, Icarus, 126, 243
Pringle J. E., 1981, ARA&A, 19, 137
Šácha J., Semerák O., 2005, Czech. J. Phys., 55, 139
Semerák O., Suková P., 2010, MNRAS, 404, 545
Shakura N. I., Sunyaev R. A., 1973, A&A, 24, 337
Stahler S. W., 1983, ApJ, 268, 155
Storzer H., 1993, A&A, 271, 25
Šubr L., Karas V., 2005, in Hledík S., Stuchlík Z., eds, Proc. RAGtime 6/7: Workshops on Black Holes and Neutron Stars, Silesian University in Opava, Czech Republic. A Manifestation of the Kozai Mechanism in the Galactic Nuclei. p. 281
Tohline J. E., Hachisu I., 1990, ApJ, 361, 394
Tresaco E., Elipe A., Riaguas A., 2011, Celest. Mech. Dyn. Astron., 111, 431
Trova A., Huré J.-M., Hersant F., 2014, A&A, 563, A132
Trova A., Schroven K., Hackmann E., Karas V., Kovář J., Slaný P., 2018, Phys. Rev. D, 97, 104019
Wisdom J., Tremaine S., 1988, AJ, 95, 925
Wong C. Y., 1973, Ann. Phys., 77, 279
Woodward J. W., Sankaran S., Tohline J. E., 1992, ApJ, 394, 248

APPENDIX A: INTEGRALS $J_{n,m}$

From Gradshteyn & Ryzhik (2007), we have

$$\int_0^{\pi/2} \cos^n\theta \sin^m\theta d\theta = \frac{1}{2} B\left(\frac{n+1}{2}, \frac{m+1}{2}\right), \tag{A1}$$

where $B(x, y) = \frac{\Gamma(x)\Gamma(y)}{\Gamma(x+y)}$ is the complete Beta function, and $\Gamma(x)$ is the Gamma function. From this expression, we can easily deduce $J_{n,m}$ (integral bounds 0 and 2π). We find

$$J_{n,m} = \frac{1}{2} B\left(\frac{n+1}{2}, \frac{m+1}{2}\right)\left[1+(-1)^n\right]\left[1+(-1)^{n+m}\right]. \tag{A2}$$

It follows that $J_{n,m} = 0$ when n is even or when $n+m$ is even (n and m have different parity). The expressions for $J_{n,m}$ are given in Table 1 for $n = \{0, 1, 2, 3, 4\}$ and $m = \{0, 1, 2, 3, 4\}$.

APPENDIX B: RESIDUAL MASS DENSITY

The residual density is found from the Poisson equation, i.e.

$$\nabla^2\left[\frac{\mathbf{K}(k)}{\sqrt{(a+R)^2+Z^2}}\right] = \frac{k_0\mathbf{K}(k_0)}{4R^2} + \left[\frac{\partial^2 k}{\partial R^2} + \frac{\partial k^2}{\partial Z^2}\right]\frac{\mathbf{E}(k_0)}{k_0'^2} + \left[\left(\frac{\partial k}{\partial R}\right)^2 + \left(\frac{\partial k}{\partial Z}\right)^2\right]\frac{(1+k_0^2)\mathbf{E}(k_0) - k_0'^2\mathbf{K}(k_0)}{kk_0'^4}, \tag{B1}$$

where the partial derivatives of $\mathbf{K}(k)$ and $\mathbf{E}(k)$ with respect to the modulus k are found in mathematical textbooks (Gradshteyn & Ryzhik 2007). By expanding all the terms inside the curly brackets, this quantity is strictly zero provided $a - R \neq 0$ and $Z \neq 0$, which never occurs in free space.

APPENDIX C: PARTIAL DERIVATIVES

There are different ways to calculate the partial derivatives of κ with respect to a and z. We find convenient to rewrite $\mathbf{K}(k)$ as the definite integral over the azimuth, i.e. equation (3). The denominator is then expanded and rearranged so that the n-order derivative with respect to a and z writes

$$\begin{aligned}\frac{\partial^n\kappa}{\partial a^{n-m}\partial z^m} &= \frac{\partial^n}{\partial a^{n-m}\partial z^m}\int_0^{\frac{\pi}{2}} \frac{d\phi}{\sqrt{\Delta^2 - 4aR\sin^2\phi}} \\ &= \int_0^{\frac{\pi}{2}} d\phi \frac{\partial^n}{\partial a^{n-m}\partial z^m}\left\{[a+R\cos(2\phi)]^2 + [R\sin(2\phi)]^2 + \zeta^2\right\}^{-1/2}.\end{aligned} \tag{C1}$$

Denoting $D = [a + R\cos(2\phi)]^2 + [R\sin(2\phi)]^2 + \zeta^2$, we have

$$\frac{\partial D^{-1/2}}{\partial a} = -[a+R\cos(2\phi)]\, D^{-3/2} \tag{C2}$$

and

$$\frac{\partial^2 D^{-1/2}}{\partial a^2} = -D^{-3/2} + 3[a+R\cos(2\phi)]^2 D^{-5/2}. \tag{C3}$$

It follows that

$$\frac{\partial\kappa}{\partial a} = \int_0^{\frac{\pi}{2}} \frac{\partial D^{-1/2}}{\partial a} d\phi = -(a+R)\Delta^{-3}\frac{\mathbf{E}(k)}{k'^2} + 2R\Delta^{-3}\frac{\mathbf{E}(k) - k'^2\mathbf{K}(k)}{k^2k'^2} \tag{C4}$$

and

$$\begin{aligned}\frac{\partial^2\kappa}{\partial a^2} &= \int_0^{\frac{\pi}{2}} \frac{\partial^2 D^{-1/2}}{\partial a^2} d\phi \\ &= -\Delta^{-3}\frac{\mathbf{E}(k)}{k'^2} + 3\Delta^{-3}\frac{\mathbf{E}(k)}{k'^2} - 3\zeta^2\Delta^{-5}\frac{2(1+k'^2)\mathbf{E}(k) - k'^2\mathbf{K}(k)}{3k'^4} - 12R^2\Delta^{-5}\frac{(1+k'^2)\mathbf{E}(k) - 2k'^2\mathbf{K}(k)}{3k^4k'^2} \\ &= 2\Delta^{-3}\frac{\mathbf{E}(k)}{k'^2} - \zeta^2\Delta^{-5}\frac{2(1+k'^2)\mathbf{E}(k) - k'^2\mathbf{K}(k)}{k'^4} - 4R^2\Delta^{-5}\frac{(1+k'^2)\mathbf{E}(k) - 2k'^2\mathbf{K}(k)}{k^4k'^2}.\end{aligned} \tag{C5}$$

For the z-derivatives, we have

$$\frac{\partial D^{-1/2}}{\partial z} = \zeta D^{-3/2}, \qquad \frac{\partial^2 D^{-1/2}}{\partial z^2} = -D^{-3/2} + 3\zeta^2 D^{-5/2} \tag{C6}$$

and, consequently,

$$\frac{\partial\kappa}{\partial z} = \zeta\int_0^{\frac{\pi}{2}} \frac{\partial D^{-1/2}}{\partial z} d\phi = \zeta\Delta^{-3}\frac{\mathbf{E}(k)}{k'^2} \tag{C7}$$

and

$$\frac{\partial^2\kappa}{\partial z^2} = \int_0^{\frac{\pi}{2}} \frac{\partial^2 D^{-1/2}}{\partial z^2} d\phi = -\Delta^{-3}\frac{\mathbf{E}(k)}{k'^2} + \zeta^2\Delta^{-5}\frac{2(1+k'^2)\mathbf{E}(k) - k'^2\mathbf{K}(k)}{k'^4}. \tag{C8}$$

APPENDIX D: F90 PROGRAM FOR THE EXTERIOR POTENTIAL

```
Program F90drivercode3
   ! ''The exterior gravitational potential of toroids''
   ! Hure, Basillais, Karas, Trova & Semerak (2019), MNRAS
   ! gfortran F90drivercode3.f90; ./a.out
   ! not optimized
   Implicit None
   Integer,Parameter::AP = Kind(1.00D + 00)
   Real(Kind=AP),Parameter::PI = ATAN(1._AP)*4
   Real(KIND = AP)::B,RC,MASS,E ! core radius, main radius and mass of the shell, and ax-
ial ratio
   Real(KIND = AP)::KMOD,KMOD2,KPRIM,KPRIM2 ! moduli
   Real(KIND = AP)::R,Z,PSI ! cylindrical coordinates and potential value where it is esti-
mated
   Real(KIND = AP)::Z2,VAL,DELTA,DELTA2,DELTA3,DELTA4,DELTA5 ! misc
   Real(KIND = AP)::KMOD4,KPRIM4,S0,S10,S20,S02,D32,S2D32,D52,S2C2D52 ! misc
   Real(KIND = AP)::ELLIPTICK,ELLIPTICE ! complete elliptic integrals
   ! ? input parameters (properties of the shell)
   B = 0.1_AP
   RC = 1._AP
   E = B/RC
   MASS = B*RC*PI**2*4
   print*,''Mass of the shell'',MASS
   ! ? values of R and Z where the potential is requested (must be outside the cavity!)
   R = RC*2
   Z = RC*2
   Z2 = Z**2
   If ((R-RC)**2 + Z2-B**2<0._AP) Then
      ! approximation not valid inside the shell
      PSI = 0._AP
   Else
      DELTA2 = (R+RC)**2 + Z2
      KMOD2 = RC*R*4/DELTA2
      DELTA = Sqrt(DELTA2)
      KPRIM2 = ((R-RC)**2 + Z2)/DELTA2
      ! values of K(k) and E(k) to be set here !
      ! ELLIPTICE =
      ! ELLIPTICK =
      !misc.
      DELTA3 = DELTA2*DELTA
      DELTA5 = DELTA3*DELTA2
      KMOD4 = KMOD2**2
      KPRIM4 = KPRIM2**2
      ! surface factors
      S0 = 1._AP
      S10 = E**2/2
      S20 = E**2/2
      S02 = S20
      ! coefficients
      D32 = ELLIPTICE/KPRIM2
      S2D32 = (ELLIPTICE-KPRIM2*ELLIPTICK)/KPRIM2/KMOD2
      D52 = ((1._AP + KPRIM2)*ELLIPTICE*2-KPRIM2*ELLIPTICK)/KPRIM4/3
      S2C2D52 = ((1._AP + KPRIM2)/KPRIM2*ELLIPTICE-ELLIPTICK*2)/KMOD4/3
      ! order 0
      VAL = ELLIPTICK/DELTA*S0
      ! order 1
```

```
      VAL = VAL+RC*(-(R+RC)*D32/DELTA3 + S2D32/DELTA3*R*2)*S10
      ! order 2
      VAL = VAL+RC**2*((-D32/DELTA3 + D32/DELTA3*3-D52*Z2/DELTA5*3-S2C2D52/DELTA5*R**2*12)*S20&
           &+(-D32/DELTA3 + D52*Z2/DELTA5*3)*S02)/2
      PSI = -VAL*B*RC*PI*8
      Print *,''Potential value (2nd-order)'',PSI,PSI/MASS*RC
   Endif
  End Program F90drivercode3
```

This paper has been typeset from a TEX/LATEX file prepared by the author.